The 7th International Symposium on Virtual Reality, Archaeology and Cultural Heritage
VAST (2006)
M. Ioannides, D. Arnold, F. Niccolucci, K. Mania (Editors)

# Terrestrial laser scanner and high-resolution camera registration through single image-based modeling

D.G. Aguilera and J. G. Lahoz

High Polytechnic School, Avila, University of Salamanca, Spain

**Abstract**

*This paper deals with an important topic: the automatic co-registration of terrestrial laser scanner data and high-resolution digital images. Our approach harnesses the power of a single image-based modeling method developed focusing on obtaining a spatial dimensional analysis from a single image. Particularly, the problem of image registration is solved automatically through a camera calibration method which takes 2D and 3D points correspondences as input data based on a search of spatial invariants: two distances and one angle.*

## 1. Introduction

### 1.1 Context

The technological development in the last years has made possible the improvement of systems for geometry and colour object's measurements. From a sensorial point of view, active and passive techniques based on terrestrial laser scanners and high-resolution cameras have monopolized this leadership respectively. Thus, the demand of 3D models for objects documentation and visualization has drastically increased. 3D modeling of close-range objects is required in manifold applications, like cultural heritage, industry, cartography, architecture, archaeology, civil engineering, medicine, and last but not least, tourism and can be accomplished with traditional image-based modeling approaches or with scanning instruments.

Particularly, the image-based modeling pipeline constitutes a very portable and low-cost technique which consists on the 3D reconstruction of objects from one or more images. In this sense, several assumptions have to be solved: from camera self-calibration and image point measurements, to 3D points cloud generation, surface extraction and texturing. In this way, image-based modeling is a technique that has undergone a big growth in the last years. This promising evolution could be portrayed by the following issues:

- New technological neighbors and new relations among these: Photogrammetry, Image Processing, Computer Graphics, Computer Vision, etc.

- New algorithms and methods have emerged in order to achieve automatization and provide new products.

On the other hand, terrestrial laser scanning methods allow to recover directly 3D measurements of the scanned scene in a few seconds, providing a high level of geometric details together with a good metric accuracy. However, up to now the 3D reconstruction of precise and reliable large objects and scenes from unorganized points clouds derived from laser scanner is a very hard problem, not completely solved and problematic in case of incomplete, noisy and sparse data. As a result, nowadays none scanner can fulfill all demands in 3D modelization projects. Although the measuring process is very fast and simple, users should be well aware that, in addition to an appropriate software, time and patience are needed to get a final result in the form of a CAD drawing or a surface representation based on a topological triangulated mesh. The high complexity of 3D modelization requires a flexible multi-input and multi-output approach able to support the information arising from different sensors/techniques and to provide different levels of information to users with different requirements [FIM*05]. In this way, the key pass through taking advance of the opportunities open by the new communication and information technologies, as well as exploit the synergies with other disciplines in order to establish specific tools.

To reinforce this need, next table (Table 1) illustrates a comparison based on the most important features with relation to laser scanning and image-based modeling methods.

| Laser Scanning | Image-based modeling |
|---|---|
| ↓ Inaccurate lines and joints | ↑ Accurate lines and joints |
| ↓ Poor colour information | ↑Good colour information |
| ↑ Prompt and accurate metric information | ↓ Hard-working and slow metric information |
| ↑ Excellent technique for the description of complex and irregular surfaces | ↓ Time-consuming technique for the description of complex and irregular surfaces |
| ↓ High-cost technique | ↑ Low-cost technique |
| ↓ The 3D model is an entity disorganized and without topology | ↑The 3D model is an entity organized and with topology |
| ↑ Light is not required to work | ↓ Light is required to work |

**Table 1:** *Comparison of features: Laser scanning vs. Image-based modeling.*

The question, which technique is 'better' than the other, cannot be answered across the board. As we can see (Table 1), each technique owns its advantages at different working fields. In many cases, a combination of both techniques might be a useful solution.

### 1.2 Related work

In this integration of techniques, where a 3D scanner is used to acquire precise geometry and a digital camera captures appearance information, the 3D model and images must be registered together in order to connect geometry and texture information.

This problem of image to model registration is closely related to the problem of camera calibration, which finds a mapping between the 3D world (object space) and a 2D image. This mapping is characterized by a rigid transformation and a camera model, also referred to as the camera's extrinsic and intrinsic parameters. This rigid body transformation takes 3D points from object space to 2D points in the camera's reference frame, and the camera model describes how these are projected onto the image plane.

The camera calibration problem is solved by matching features in the 3D model with features in the image. These features are usually points, lines or special designed objects that are placed in the scene. The matching process can be automatic or user driven, and the number of feature pairs required will depend on whether we are solving for the intrinsic, extrinsic or both parameters sets.

In the context of image registration for 3D modeling using dense laser scanner data, several approaches have been developed up to now.

A pre-calibration of camera which allows to integrate geometry and texture avoiding any user post-processing used for the Digital Michelangelo project [LPC*00], or the approach described by [RCM*99] where the image to model registration is done manually by a user who selects corresponding pairs of points. Both approaches are applied in a context of small object modeling.

In search of an automatic method, [LHS01] develop an image registration approach based on silhouette matching, where the contour of a rendered version of the object is matched against the silhouette of the object in the image. No user intervention is required, but their method is limited to cases where a single image completely captures the object.

In other scale of methods applied to large distances, dealing with outdoor scenes and based on locating invariant image features, [MNP*99] suggest correlating edges common to the color image and the range map's intensity component. [Els98] aligns images by matching up the corners of planar surfaces. More recently, [SA01] present an automatic method for image to model registration of urban scenes, where 3D lines are extracted from the point clouds of buildings and matched against edges extracted from the images. [INN*03] in their Great Buddha work, use reflectance edges obtained form the 3D points and match them against edges in the image to obtain the camera position. Finally, [ATS*03] present a novel method for 2D to 3D texture mapping using shadows as cues. They pose registration of 2D images with the 3D model as an optimization problem that uses knowledge of the Sun's position to estimate shadows in a scene, and use the shadows produced as a cue to refine the registration parameters.

In a similar context, our approach harnesses the power of a single image-based modeling method developed in [Agu05] focusing on obtaining a spatial dimensional analysis from a single image. Particularly, the problem of image registration is solved automatically through Tsai calibration algorithm [Tsa89] which takes 2D and 3D points correspondences as input data based on a search of spatial invariants: two distances and one angle.

## 2. Multi-sensor description

The Trimble GS200 laser scanner (Figure 1) was employed for the scanning process. This scanning system is provided with a rotating head and two inner high speed rotating mirrors that allow to acquire a scene

with a large enough field of view, i.e. 360º H x 60º V, reducing the need of using lots of scan stations. The sensor accuracy is below 1.5mm at 50m of distance with a beam diameter of 3mm. Furthermore, the laser allows to acquire reflected beam intensity and RGB colours.

A high-resolution camera, Nikon D70 (Figure 1), was used to overcome the poor colour information obtained from terrestrial laser scanner.

**Figure 1:** *Trimble GS200 laser scanner and digital camera, Nikon D70.*

## 3. Multi-sensor registration through single image-based modeling

A hierarchical process supported by single image-based modeling has been developed in order to register high-resolution images with laser scanner models. Nevertheless, before a 3D model can be texture mapped with a colour image, the transformation that aligns the two datasets must be estimated, which is not an easy task. The registration process is difficult to automate because image and laser points cloud are dataset which arise from sensors with different features: from its own intrinsic characteristics to features like its resolution and field of view.

The main contribution of this paper is the adaptation of a single image-based modeling approach in order to obtain geometrical constraints and a spatial dimensional analysis, which allow performing image to laser model registration automatically.
Our approach exploits vanishing points geometry inherent in oblique images as well as some geometrical constraints typical in architectural scenes. Particularly, four main steps are resolved sequentially: the first step involves an image analysis procedure based on recognition, extraction and labeling of features (special targets and vanishing lines); the second step involves the estimation of camera calibration exploiting vanishing points geometry; the third step carries out a dimensional analysis derived from a single image. This step uses the estimation of camera calibration, as well as some geometrical constraints used in single image-based modeling. Finally, the fourth step involves a search of correspondences between both dataset (3D points cloud and 2D image points) based on analyzing spatial invariants between special targets. This last step provides image to model registration together with a camera calibration tuning.

Nevertheless, this approach is only successful in a given domain where the following assumptions have to be considered:

a) The method is applicable in scenes with strong geometric contents such as architectural scenes.

b) The images acquired by digital camera have to be oblique with at least two vanishing points.

c) Special planar targets (Figure 4) are used as landmarks and have to be fixed to the building facades.

d) In order to have a primary camera pose estimation from a single view, user must know some priori information about the object (i.e. a distance) which performs as the reference frame.

The following scheme (Figure 2) aims to illustrate the methodology that we have developed in order to obtain multi-sensor registration through single image-based modeling automatically.

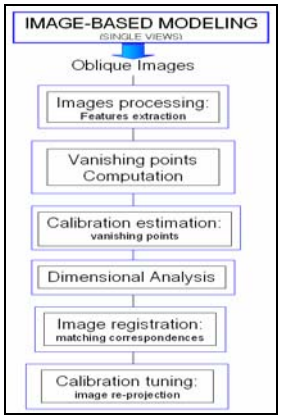


**Figure 2:** ***Multi-sensor registration through single image-based modeling.***

### 3.1 Image processing: Features extraction

A hybrid image processing step which integrates lines (vanishing lines) and interest points (special planar targets) extraction is accomplished.
With relation to vanishing lines extraction, a hierarchical method divided into two levels is applied. In the first level, linear segments are detected applying Canny filter

[Can68] and a linear regression based on least square which combines RANSAC estimator [FB81]; in the second level, segments are clustered through an iterative process based on their colinearity, taking an orthogonal distance as input parameter or threshold. Nevertheless, the presence of mini-segments could carry some problems in the clustering process, i.e. leaving unclassified vanishing lines. In this sense, a weight factor for the line coverage has been considered, which depends on the number of collinear segments as well as their length.

Regarding to the extraction of special planar targets, a seed of the planar target will be required in order to perform a cross-correlation template matching method. The probable target candidates are searched all over the high resolution image using a cross-correlation template matching method. A sub-sampled version of the high resolution image is used to decrease the computational expense. The window size is selected as 10x10 pixels. Only those pixels that have cross-correlation values greater than a predefined threshold value are defined as the target candidates. The algorithm starts searching the most probable target candidates all over the image using cross-correlation values. The seed used in the cross-correlation procedure is generated artificially according to the real target shape (Figure 3). Obviously, the presence of outliers will carry that more targets than the real number will be detected. In this sense, the own radiometric and geometric characteristics of the targets such as green background and circular shape allow filtering some of these anomalies. Finally, with the filtered candidates circular shapes will be extracted through the Generalized Hough Transform (GHT) [Bal81]. This method is a generalization of the traditional Hough transform and allows detecting basic shapes independently of the rotation and scale of the image, event pretty common when we work with oblique images.

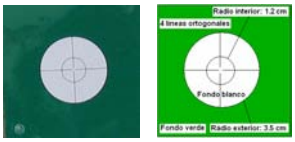


**Figure 3:** *Special planar targets.*

### 3.2 Vanishing points computation

The motivation and usefulness of precise and reliable determination of vanishing points, among other structural elements belonging to oblique images, has been demonstrated based on their correspondence with the three main orthogonal directions. Particularly, in architectural environments vanishing points provide three independent geometrical constraints which can be exploited in several ways: from the camera self-calibration and a dimensional analysis of the object to its partial 3D reconstruction.

Our vanishing points method takes a scientific approach which combines several proven methods supported by robust and statistical techniques. In this sense, the key differences of this method in relation with others approaches are reflected in the following steps:

A *Clustering step*, which cluster the mini-segments in vanishing lines.

An *Estimation step*, which applies a modification of the Gaussian sphere method [Bar83], in order to obtain an estimation of vanishing points and reject possible erroneous vanishing lines.

A *Computation step*, which applies a re-weighted least square adjustment support by M-estimators [Dom00].

More details about this new vanishing points method are described in [Agu05].

### 3.3 Calibration estimation: vanishing points

Our approach is similar to another approach [CT90] who exploiting vanishing points geometry recovers the projection matrices directly. However, in our case the method developed, uses simple properties of vanishing points adding some geometrical constraints derived from image processing step.

The camera model can be recovered following two steps, in which internal and external parameters are estimated separately.

In the first step, the intrinsic parameters, that is, the focal length, the location of the intersection between the optical axis and the image plane and the radial lens distortion, are recovered automatically based on vanishing points geometry and image processing. In the second step, the extrinsic parameters, that is, the rotation matrix and the translation vector which describe the rigid motion of the coordinate system fixed in the camera are estimated in a double process. Firstly, the rotation matrix, that is, camera orientation is obtained directly based on the correspondence between the vanishing points and the three main object directions. This relationship allows to extract the cosine vectors of optical axis, obtaining directly the three angles (axis, tilt, swing). Then, the translation vector, that is, the relative camera pose is estimated based on some priori object information, i.e. a distance, together with a geometric constraint defined by the user. Thus, the reference frame for the camera pose estimation is defined with relation to the object geometry arbitrarily.

The robustness of the method depends on the reliability and accuracy of vanishing points computation, so the incorporation of robust M-estimators in the step before is crucial.

### 3.4 Dimensional analysis

With the estimation of camera model and with the geometrical constraints defined by the user, an automatic dimensional spatial analysis based on distances and angles is performed between all possible targets combinations. Thus, for each target extracted in image processing step we compute the distances and angles with the remainder targets.

This approach is supported by constrained colinearity condition (3.1) (3.2) and trigonometric functions (3.3), which allow to obtain spatial distances and angles between whatever detected target:

$$\begin{aligned} w(1) &= r_{11}(x_1 - x_{PP}) + r_{21}(y_1 - y_{PP}) - r_{31}(f) \\ w(2) &= r_{12}(x_1 - x_{PP}) + r_{22}(y_1 - y_{PP}) - r_{32}(f) \\ w(3) &= r_{13}(x_1 - x_{PP}) + r_{23}(y_1 - y_{PP}) - r_{33}(f) \\ w(4) &= r_{11}(x_2 - x_{PP}) + r_{21}(y_2 - y_{PP}) - r_{31}(f) \\ w(5) &= r_{12}(x_2 - x_{PP}) + r_{22}(y_2 - y_{PP}) - r_{32}(f) \\ w(6) &= r_{13}(x_2 - x_{PP}) + r_{23}(y_2 - y_{PP}) - r_{33}(f) \end{aligned} \tag{3.1}$$

where, *w(1)..w(6)* are auxiliary functions derived from colinearity condition, $r_{11}...r_{33}$ is the rotation matrix coefficients, *x,y* are image coordinates, $x_{pp}$,$y_{pp}$ are principal point coordinates and *f* is the focal length.

$$\begin{aligned} X_S &= X - \left( \frac{w(2)}{w(1)} \cdot \left( \frac{DT_{XZ}}{\sqrt{\left(\frac{w(5)}{w(4)} - \frac{w(2)}{w(1)}\right)^2 + \left(\frac{w(6)}{w(4)} - \frac{w(3)}{w(1)}\right)^2}} \right) \right) \\ Y_S &= Y - \left( \left( \frac{DT_{XZ}}{\sqrt{\left(\frac{w(5)}{w(4)} - \frac{w(2)}{w(1)}\right)^2 + \left(\frac{w(6)}{w(4)} - \frac{w(3)}{w(1)}\right)^2}} \right) \right) \\ Z_S &= Z - \left( \frac{w(3)}{w(1)} \cdot \left( \frac{DT_{XZ}}{\sqrt{\left(\frac{w(5)}{w(4)} - \frac{w(2)}{w(1)}\right)^2 + \left(\frac{w(6)}{w(4)} - \frac{w(3)}{w(1)}\right)^2}} \right) \right) \end{aligned} \tag{3.2}$$

where, $X_S$, $Y_S$, $Z_S$ are the viewpoint coordinates, *X, Y, Z* are the ground point coordinates and *DT* is the spatial distance that we want to compute.

With relation to trigonometric functions, for a triangle in the Euclidean plane with edges *a*, *b*, *c* and opposite angles $\alpha$, $\beta$, $\gamma$, the following holds:

$$\begin{aligned} a^2 &= b^2 + c^2 - 2bc\cos\alpha; b^2 = a^2 + c^2 - 2ac\cos\beta \\ c^2 &= a^2 + b^2 - 2ab\cos\gamma \end{aligned} \tag{3.3}$$

The accuracy of the method taking into account the inherent conditions in a single image-based modeling approach is around ±10 cm. Nevertheless, this is not especially crucial since we consider that special targets are enough separate each others. So, in most of the cases, a global approximation is usually enough for a search of correspondences.

### 3.5 Image registration: matching correspondences

This step presents a technique to perform an automatic matching between 3D and 2D points (special targets) belonging to laser model and high-resolution images respectively.

The solution that we propose is based on the invariants properties of two distances and one angle, which are translational and rotational invariant parameters independently of the sensor viewpoint. Furthermore, three of the angle/distance elements, in which at least one of them must be distance, can exactly define a triangle. Therefore, the presented search scheme is the same as to find the equal 3D triangles in both point sets. This search will serve also for rejecting possible outliers. Those points whose correspondence of invariants or triangles is not found of will not be considered. In the end, a final list with the correspondences of target points will be obtained which will constitute the input data in the calibration tuning process.

The method developed for establishing correspondences between both datasets relies on the approach developed by [Akc03], who in order to materialize the correspondence between two laser scanner datasets develops a search of invariants supported by two distances and one angle. Nevertheless, Acka works directly with two homogeneous datasets, which proceed to the same sensor, and with a previous measurement of the invariants obtained through surveying techniques. In the approach presented here, a correspondence between two heterogeneous datasets (2D image points and 3D laser points) is established.

In order to search homologous points, all possible space angles and distances are calculated in both datasets, one through the single image-based modelling approach proposed before and the other directly through 3D coordinates extracted from laser points cloud. The total computational cost for the distances and angles is given below (3.4):

$$C\binom{Ni}{2} + C\binom{Nc}{2} + Ni \cdot C\binom{Ni-1}{2} + Nc \cdot C\binom{Nc-1}{2} \tag{3.4}$$

where, *Ni* is the number of points in the candidate image target list and *Nc* is the number of points in the laser target list, and *C* stands for the combination operator.

Every space angle and two distance combinations for each point in the image target candidate list is searched in the target laser list with a predefined angle/distance threshold values (i.e. angle <0.5º, distance <15cm). Three of the angle/distance elements, in which at least one of them must be distance, can exactly define a triangle. Therefore, the presented search scheme is the same as to find the equal 3D triangles in the both point sets. If a point does not have a compatible 3D triangle in the invariants list, this point does not have a label, namely this point as a wrong target candidate, and must be discarded from the candidate target image list.

### 3.6 Calibration tuning: image re-projection

A Tsai camera calibration technique [Tsa89] is used to obtain a calibration tuning, especially the image registration with relation to laser scanner. Its implementation needs correspondences between both datasets: 3D laser points and 2D image points. Tsai's technique uses a two-stage approach to compute: first, the position and orientation and, second, the internal parameters of the camera. Thus, Tsai's approach offers the possibility to calibrate internal and external parameters separately. This option is particularly useful in our case, since the single image-based modeling method developed allows us to known these parameters with a similar strategy.

Depending on internal parameters accuracy, we carry out one or two stage approach of Tsai's camera calibration. So, if good accuracy has been achieved through single image-based modeling method, a minimal number of 5 points will be used to compute the camera pose. Furthermore, the three known rotations angles perform as initial approximations in the algorithm.

Due to the different nature of the sensors, as well as the own characteristics of the single image-based modeling approach, a single run of the algorithm can lead to a camera registration that is not fully satisfactory. To improve the accuracy and reliability of the calibration process, an iterative procedure has been introduced. In this sense, each 3D point detected as special target in the points cloud will be re-projected over the image based on colinearity condition principles and the computed camera parameters. Small discrepancies remain between the projected 3D points and the original extracted image points. The 3D coordinates of the laser scanner and the re-projected corresponding image points constitute the input to compute a new calibration. This iterative process follow until the Euclidean distance between the re-projected points and the original image targets points will be minimized (threshold distance). The general idea is that at each iteration the distance between the two datasets is reduced, allowing a better computation of camera parameters.

To ensure the convergence of the algorithm and the improvement of the initial camera model estimation, the calibration error of each correspondence is computed and recorded. In each new iteration, only matching pairs for which the calibration error decreases are updated, and the other are kept unchanged. In this stage, no robust estimation is used since the step before ensures that no outliers are present within the correspondences.

After the calibration tuning procedure based on this technique, a full model for the camera with relation to laser scanner is available and ready to map textures.

## 4. Experimental results

We have validated our approach on several different datasets, but we only present the experimental results tested over an emblematic romanic church situated in Avila (Spain), San Pedro's church (Figure 4).

**Figure 4:** *Original image with special targets (3008x2000 pixels)*

After applying the image processing step, we obtain the different features extracted with sub-pixel accuracy (Figure 5).

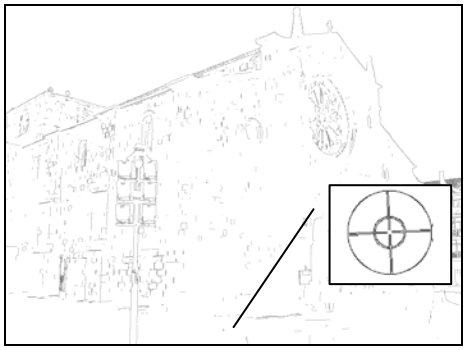

**Figure 5:** *Image features extraction.*

With relation to the features statistics (Table 2):

| | |
|---|---|
| Vanishing Lines | 231 segments clustered in X direction<br>274 segments clustered in Y direction<br>35 segments clustered in Z direction<br>91 segments clustered as outliers |
| Special Targets | 20 targets were detected<br>2 targets were not detected<br>7 targets were detected as outliers |
| Accuracy ($\sigma$) | 0.5 pixels |

**Table 2:** *Statistics in features extraction.*

Next, a robust method for vanishing points computation which combines Danish M-estimator together with Gaussian Sphere was applied iteratively (Table 3).

**Vanishing points computation** ($4^{th}$ iteration)

| **Gauss Sphere +Danish est.** (Unit: pixels) | **VPX** | **VPY** | **VPZ** |
|---|---|---|---|
| **x** | 3761.981 | -1483.7 | 1054.8 |
| **y** | 1432.395 | 1255.76 | -2378.6 |
| $\sigma_{xx}$ | 0.13 | 0.35 | 0.38 |
| $\sigma_{yy}$ | 0.18 | 0.40 | 0.57 |

**Table 3:** *Vanishing points computation.*

With the structural support provided by vanishing points an estimation of camera calibration parameters was obtained (Table 4):

**Camera calibration estimation:** vanishing points

| **Internal Parameters** (Unit: millimetres) | | **External Parameters** (Unit: degrees, metres) | |
|---|---|---|---|
| **PP [x]** | 11.83 | **Axis**: 38.00 | **X**: -14.95 |
| **PP [y]** | 7.76 | **Tilt**: 95.80 | **Y**: -12.03 |
| **Focal** | 18.10 | **Swing**: 181.44 | **Z**: 1.7 |
| $K_1$ | 0.003245 | | |
| $K_2$ | -0.00001 | | |

| **Internal Parameters** (Unit: millimetres) | | **External Parameters** (Unit: radian, metres) | |
|---|---|---|---|
| $\sigma_{PP}$ **[x]** | 0.032 | $\sigma_{Axis}$: 0.00175 | $\sigma_X$: -0.034 |
| $\sigma_{PP}$ **[y]** | 0.036 | $\sigma_{Tilt}$: 0.00213 | $\sigma_Y$: 0.039 |
| $\sigma_F$ | 0.044 | $\sigma_{Swing}$: 0.00127 | $\sigma_Z$: -0.048 |
| $\sigma_{K1}$ | 0.000134 | | |
| $\sigma_{K2}$ | 0.000001 | | |

**Table 4:** *Camera calibration estimation.*

**Dimensional analysis:** single image-based modeling

Taking into account the threshold fixed to distances and angles: 15cm and 0.5º respectively, every space angle and two distances combinations for each point in the image target candidate list was searched in the target laser list, obtaining the following:

- 7 correspondences were located between both datasets and added to the target image list.

- 6 especial targets were detected as outliers being discarded from the candidate target image list.

In the laser scanning context, all special targets were correctly extracted by laser scanner software, so eleven 3D points were added to the laser points list (Figure 6).

**Figure 6:** *Laser model and the special targets extracted.*

Finally, once both datasets were matched each other in image and laser list, a camera calibration tuning with seven correspondences was performed in order to provide an image to laser model registration (Table 5).

**Camera calibration tuning:** image to laser model registration

| **Image to laser model registration** (5th iteration) (Units: degrees, radian and metres) | |
|---|---|
| **Axis**: 38.6257; $\sigma_A$: 0.00065 | **X**: 8.138; $\sigma_X$: -0.009 |
| **Tilt**: 95.667; $\sigma_T$: 0.00023 | **Y**: -3.307; $\sigma_Y$: 0.012 |
| **Swing**: 181.9487; $\sigma_S$: 0.00077 | **Z**: 1.094; $\sigma_Z$: -0.021 |

**Table 5:** *Calibration tuning: image registration.*

A re-projection strategy (section 3.6) based on five iterations was necessary to minimize the Euclidean distance between matched points, obtaining good results in mapping textures (Figure 7).

**Figure 7:** *Multi-sensor registration: mapping textures.*

## 5. Conclusions and future perspectives

We have developed a method for registering high-resolution images to laser models. Our technique uses a single image-based modeling approach which provides relevant data: from camera calibration and geometrical constraints to a metric dimensional analysis. Particularly, in the automatic co-registration of terrestrial laser scanner data and single digital images, our approach performs a dimensional analysis from a single image based on a search of spatial invariants: two distances and one angle. This approach works very well for outdoors scenes in which the geometry of the building is easy to modeling. Nevertheless, some ill aspects have been assessed: In the search of correspondences step, maybe applying an adaptative threshold supported by a RANSAC estimator could be a good idea to reject fewer points. Obviously, a large sensor's baseline does not contribute in a good way to map textures, obtaining some anomalies in upper parts of the building.

With relation to future perspectives, the research could be extend to exploit the single image-based modeling towards applications related with the improvement and refinement of the laser model, adding metric and semantic information in missing areas (non reflective material, occlusions, shadows, etc). Furthermore, in the context of texture mapping, develop algorithms that allow to handle the resulting problem of occlusions, illumination properties and transition between junctions, would let to achieve a realistic and integral representation of the object.

## References

[Agu05] AGUILERA D. G., 2005. Doctoral Thesis. University of Salamanca.

[Akc03] AKCA DEVRIM, 2003: Full automatic registration of laser scanner point clouds. ETH Zurich.

[ATS*03] P. K. ALLEN, A. TROCCOLI, B. SMITH*. New methods for digital modeling of historic sites. IEEE

[Bal81] BALLARD D. Generalized Hough transform to detect arbitrary patterns, 1981. IEEE, 13(2):111-122.

[Can86] CANNY J.F. 1986. A computational approach to edge detection. IEEE journal.

[CT90] CAPRILE B. and TORRE V. 1990. Using vanishing points for camera calibration. IJCV 4 (29).

[Dom00] DOMINGO PRECIADO ANA, 2000. Tesis Doctoral. Universidad de Cantabria.

[Els98] M. D. ELSTROM. Master's thesis, University of Tennessee, Knoxville, 1998.

[FIM*05] FINAT CODÉS J*: The roman theatre of Clvnia: hybrid strategies. ISPRS Workshop Italy.

[FB81] FISCHLER, M. A., and R. C. BOLLES, 1981. Random sample consensus. CM Communications.

[INN*03] IKEUCHI, NAKAZAWA,*. Creating virtual buddha statues through observation. IEEE Workshop.

[LHS01] H. P. LENSCH, W. HEIDRICH*. A silhouette-based algorithm for texture registration and stitching, Graphical Models, vol. 63, n4.

[LPC*00] M. LEVOY, K. PULLI, B. CURLESS,*, The digital Michelangelo project: 3D scanning of large statues. Siggraph, CG Proceedings, 2000.

[MNP*99] MCALLISTER, L. NYLAND, V. POPESCU,*. Eurographics Rendering Workshop, 1999.

[RCM*99] C. ROCCHINI, P. CIGNOMI, C. MONTANI,*, "Multiple textures stitching and blending on 3D objects,". Eurographics, New York, 1999.

[SA01] I. STAMOS and P. K. ALLEN. Automatic registration of 2-D with 3-D imagery in urban environments. Proceedings ICCV-01, 2001.

[Tsa89] TSAI Y., 1989. Synopsis of recent progress on camera calibration for 3d machine vision. Robotics Rew.